Available online at www.sciencedirect.com
SCIENCE DIRECT
Analytical Biochemistry 348 (2006) 94–104
ANALYTICAL BIOCHEMISTRY
www.elsevier.com/locate/yabio

# Ligand binding to one-dimensional lattice-like macromolecules: Analysis of the McGhee–von Hippel theory implemented in isothermal titration calorimetry

Adrián Velázquez-Campoy *

*Institute of Biocomputation and Complex Systems Physics (BIFI), Universidad de Zaragoza, Corona de Aragón 42, E-50009 Zaragoza, Spain*

Received 29 July 2005
Available online 26 October 2005

**Abstract**

The theory developed by McGhee and von Hippel for ligand binding to a one-dimensional lattice-like macromolecule provides a closed analytical form in the Scatchard representation. The application of such theory has been complicated by two facts: (1) it has been practically reduced to binding techniques, such as equilibrium dialysis, in which the partition between bound and free concentrations of all reactant species are directly accessible and experimentally determined, but infrequently applied to other binding techniques, such as calorimetry or spectroscopy, in which the direct observable is a magnitude proportional to the advance of the binding reaction monitored along the titration experiment, and (2) Scatchard analysis, developed as a quantitative graphical method, is currently outdated and used only qualitatively because of its weaknesses, limitations, and deficiencies. However, a general exact method for applying such theory to titration techniques in a correct and precise manner, without any limitation, can be delineated. In this article, the theory of cooperative ligand binding to linear lattice-like macromolecules has been implemented in isothermal titration calorimetry for the first time. This technique provides a complete thermodynamic characterization of ligand binding, but it has been barely used properly for this type of system. The description, the analysis of the formalism, and practical guidelines are presented, with considerations for experimental design and data analysis.


*Keywords:* McGhee-von Hippel theory; Isothermal titration calorimetry; Ligand binding; Numerical methods

Nonspecific ligand binding to a lattice-like macromolecule, such as a nucleic acid or a carbohydrate, is common in nature. The macromolecule can be considered a mono-dimensional lattice with $N$ potential binding sites homogeneously distributed and constituted by repeating units, and any bound ligand molecule occupies a certain number of repeating units, $l$. The geometric properties of the system, that is, $N$, the number of repeating units per macromolecule, and $l$, the length of the ligand (in a macromolecule repeating unit basis), in addition to the thermodynamic binding parameters, govern the behavior of the system.

The number of ligand molecules bound per macromolecule, $v$, is the main descriptor of the behavior of the system under study and it is defined as

$$v = \frac{[\mathrm{L}]_\mathrm{B}}{[\mathrm{M}]_\mathrm{T}}, \tag{1}$$

where $[\mathrm{L}]_\mathrm{B}$ is the concentration of bound ligand and $[\mathrm{M}]_\mathrm{T}$ is the total concentration of macromolecule. The limiting values for the binding parameter are 0 and $N/l$, thus, reflecting the degree of saturation of the macromolecule. The terminology and the definition of the variables followed in [1] have been adopted in this article because of its parallelism with the traditional approach for macromolecules with several nonoverlapping binding sites. Other authors prefer using the binding density

$$v = \frac{[\mathrm{L}]_\mathrm{B}}{N[\mathrm{M}]_\mathrm{T}}, \tag{2}$$

* Fax: +34 976 562215.
*E-mail address:* adrianvc@unizar.es.

0003-2697/$ - see front matter © 2005 Elsevier Inc. All rights reserved.
doi:10.1016/j.ab.2005.10.013

which represents the saturation fraction of each repeating unit in the macromolecule and presents limiting values of 0 and $1/l$. Therefore, the only difference between these two approaches is just a factor of $1/N$.

Traditionally, binding equilibrium equations have been transformed from the hyperbolic representation ($v$ versus [L]), which would require nonlinear regression analysis, into a transformed representation to facilitate the interpretation and analysis. One of these transformations is the Scatchard plot [2]. In this approach, $v/[L]$ is represented as a function of $v$

$$\frac{v}{[L]} = f(v; N, l, k), \tag{3}$$

where $k$ is the microscopic dissociation constant of each binding site. In the case of a macromolecule with $N$ equivalent and independent binding sites and a ligand with size $l = 1$, it corresponds to a linear plot, but in the case of several classes of binding sites, or interacting binding sites, or a ligand with size $l > 1$, it corresponds to a curved plot. Therefore, for a ligand of size $l > 1$ the traditional approach does not apply and the equilibrium behavior of the system differs significantly from the case in which $l = 1$. McGhee and von Hippel [3,4] first derived a closed form for the Scatchard representation valid for any ligand size, $l$, any ligand dissociation constant, $k$, and any level of cooperativity interaction between ligands bound contiguously, $\omega$, for infinite homogeneous lattices

$$\frac{v}{[L]} = f(v; N, l, k, \omega). \tag{4}$$

For a detailed description of the methodology and the data analysis for this type of system, see [5]. Extensions of this theory have been developed for finite lattices [6,7], heterogeneous systems in which the binding sites are not homogeneously distributed throughout the macromolecule [8], different classes of binding sites present in the macromolecule [7], different ligand binding modes [6,9,10], a mixture of different ligands which could be used in displacement experiments [1], or an allosteric binding model [11,12].

The purpose of this work is to analyze the implementation of this theory in isothermal titration calorimetry (ITC)[1]. The problem of determining how the ligand binds (e.g., assessing the possibility of different binding modes) or establishing the model to be applied is not the goal of this work [13,14], and it will be assumed that ligand binding follows the McGhee–von Hippel theory. The method is valid for ligands with any binding affinity, any size (in macromolecule repeating unit basis), and any level of cooperativity. ITC presents a great advantage over spectroscopic techniques: the possibility of determining simultaneously the affinity, $k$, and the enthalpy of binding, $\Delta H$. Therefore, it is possible to perform a complete characterization of the binding process (determination of affinity, Gibbs energy, enthalpy and entropy of binding) in just one experiment. Both spectroscopy and calorimetry allow evaluating the binding affinity, which determines the advance of the reaction because it governs the partition into free and bound species. Additionally, calorimetry provides the binding enthalpy, an additional binding parameter that is important in describing the intermolecular driving interactions underlying the binding process, and it can be of help when discriminating between different cases, as will be seen later. Detailed descriptions of the technique, its applications, and standard methodology and analysis can be found elsewhere [15–24]. Despite the widespread recognition of ITC as an excellent tool for studying biomolecular reactions, it has been scarcely applied to lattice-like macromolecular systems, its full potential has not been completely exploited [7,25–32], and it has very few times been used properly [7,27–29,31].

To date no implementation of the theory for cooperative binding has been done. McGhee and von Hippel derived two different equations for each of the two possible situations: independent binding ($\omega = 1$) and cooperative binding ($\omega \neq 1$). The latter equation cannot be applied in the case of noncooperative binding because it diverges when $\omega$ equals unity. Some authors have developed a single equation valid for any level of cooperativity ($\omega = 1$ and $\omega \neq 1$), thus, eliminating the need of a different expression for each case [33,34]. However, as will be shown below, the implementation of the theory in isothermal titration calorimetry still requires the use of the partial binding parameters, and no single expressions valid for any cooperativity level have been developed for them. Therefore, two situations will be considered: independent binding and cooperative binding.

## Case I. Lineal lattice-like macromolecule with noncooperative ligand binding: macromolecule with $N$ equivalent and independent binding sites and ligand size $l \geqslant 1$

McGhee and von Hippel [3,4] derived a closed analytical expression for the binding parameter in the Scatchard representation in the case of a homogeneous mono-dimensional lattice-like macromolecule with $N$ independent binding sites and ligand with size $l (l \geqslant 1)$

$$\frac{v}{[L]} = \frac{N - lv}{k}\left(\frac{N - lv}{N - (l-1)v}\right)^{l-1}. \tag{5}$$

This equation was derived assuming an infinite lattice; however, real macromolecules are not infinite and end-effects will arise. The error in using such equation is estimated to be less than the experimental error as long as $N/l > 30$. However, using an expression valid for finite lattices that includes the correction factor $(N - l + 1)/N$ in Eq. (5) [7] or employing an exact combinatorial analysis for finite lattices [6], it has been demonstrated that the infinite lattice approximation is a reasonably good approach even in cases where $N/l$ is significantly lower than 30.

Eq. (5) is linear in $v$ only if $l = 1$. If $l > 1$, due to the presence of the additional factor in the right hand of Eq. (5),

[1] *Abbreviation used*: ITC, isothermal titration calorimetry.

the Scatchard plot always lies beneath the linear plot corresponding to $l = 1$, exhibiting positive curvature and reflecting an apparent negative cooperativity between ligands (usually named "entropic resistance to saturation") easily explained from a statistical basis. As binding proceeds to saturation, it is more difficult to find $l$ free consecutive binding sites when $l$ is large. Then, the larger the ligand size $l$, the larger such effect.

To eliminate [L] from Eq. (5), it can be rewritten expressing [L] in terms of total concentrations of macromolecule and ligand

$$\frac{v}{[\mathrm{L}]_\mathrm{T} - [\mathrm{M}]_\mathrm{T} v} = \frac{N - lv}{k}\left(\frac{N - lv}{N - (l-1)v}\right)^{l-1}. \tag{6}$$

This equation can be rewritten as

$$\left([\mathrm{L}]_\mathrm{T} - [\mathrm{M}]_\mathrm{T} v\right)(N - lv)^l - kv(N - (l-1)v)^{l-1} = 0, \tag{7}$$

which corresponds to an $(l+1)$-order polynomial equation. For any given values for $[\mathrm{L}]_\mathrm{T}$, $[\mathrm{M}]_\mathrm{T}$, and $k$, a root with physical meaning (i.e., positive and lower than $N/l$) can be determined. The Newton–Raphson method is very simple to implement and convergence is extremely fast [35]. Considering the equation we need to solve (Eq. (7))

$$F(v) = 0, \tag{8}$$

a recursive sequence $\{v_\mathrm{n}\}$ is generated

$$v_{n+1} = v_n - \frac{F(v_n)}{F'(v_n)}, \tag{9}$$

starting with an appropriate value for $v_0$ (e.g., $v_0 = 0$ or $v_0 = 0.05 \times N/l$). Care should be taken to avoid the problem arising if the derivative of the function $F(v)$ vanishes within the interval. The root is given by the limit of the sequence when n approaches infinity, but, in practice, the iteration procedure is continued until the convergence criterion is fulfilled

$$|v_{\mathrm{n}+1} - v_n| < \varepsilon, \tag{10}$$

where the parameter $\varepsilon$ is given a low enough value (e.g., $\varepsilon = 10^{-12}$). According to calculations, for any given values of $N$, $l$, $[\mathrm{L}]_\mathrm{T}$, $[\mathrm{M}]_\mathrm{T}$, and $k$, the correct root is obtained in less than 30 iterations with the selected accuracy. To avoid errors due to big numbers in the numerator and the denominator in the second term of Eq. (9), the actual function used to find the root was not $F(v)$, but a modified function introducing the constant scaling factor $N^{-(l-2)}$ which does not change the localization of the roots.

In isothermal titration calorimetry the heat associated with a binding process is measured. The instrument performs a series of injections of a ligand solution from a computer-controlled syringe into a macromolecule solution placed in a thermostatized cell and the heat effect associated with each injection, due to the binding event (and other heat effects related to secondary phenomena that can be subtracted out conveniently), is measured. The total concentration of each reactant in the cell after injection $i$ is

$$[\mathrm{M}]_{\mathrm{T},i} = [\mathrm{M}]_0\left(1 - \frac{v}{V}\right)^{\mathrm{i}} \text{ and } [L]_{\mathrm{T},i} = [\mathrm{L}]_0\left(1 - \left(1 - \frac{v}{V}\right)^{i}\right), \tag{11}$$

where $[\mathrm{M}]_0$ and $[\mathrm{L}]_0$ are the initial concentrations of macromolecule in the calorimetric cell and the ligand in the syringe, v is the injection volume, and $V$ is the cell volume. From that, knowing $[\mathrm{M}]_{\mathrm{T},i}$ and $[\mathrm{L}]_{\mathrm{T},i}$ and assuming values for $N$, $l$, and $k$, it is possible to determine the binding number after each injection, $v_i$, solving Eq. (7) appropriately. Then, the heat effect associated with injection, $q_i$, can be evaluated as follows:

$$q_i = V\Delta H\left([\mathrm{M}]_{\mathrm{T},i} v_i - \left(1 - \frac{v}{V}\right)[\mathrm{M}]_{\mathrm{T},i-1} v_{i-1}\right). \tag{12}$$

Eq. (12) is used in a nonlinear regression procedure to extract the optimal values of the thermodynamic parameters $N$, $l$, $k$, and $\Delta H$ from the experimental data.

Fig. 1 shows the simulated titration corresponding to a macromolecule with $N = 100$ binding sites and a ligand with size $l = 3$. Although the thermogram and the titration plot (Fig. 1A) look similar to the result obtained for a system with ligand size $l = 1$, there exist some significant differences. Considering the values used for $N$ and $l$, the expected maximal number of ligand molecules bound per macromolecule or stoichiometry is $N/l = 100/3 \approx 33.3$. However, the apparent maximal binding number, inferred from the localization of the inflection point of the titration plot, is around 30. The larger the ligand size, the larger the difference between the apparent and the actual maximal binding numbers. Therefore, if the data analysis is performed with a model for a ligand with size $l = 1$ [30,32], then, both the maximal binding number and the binding affinity will be estimated with a significant error (the values from the fitting using a model considering a ligand size $l = 1$ are $N = 30.5$, $k = 2 \cdot 10^{-5}$ M, and $\Delta H = 10.3$ kcal/mol; whereas the values used for that calculation were $N = 100$, $l = 3$, $N/L = 33.3$, $k = 10^{-5}$ M, and $\Delta H = 10$ kcal/mol). The binding enthalpy is more accurately estimated, because it is practically model independent and it is mainly determined by the difference between the low saturation region and the high saturation region in the titration plot, depending almost exclusively on the number of moles of ligand injected at each injection. When planning an experiment, a concentration of ligand high enough to reach saturation in a reasonable number of injections should be considered. For a macromolecule with $N$ binding sites and a ligand with size $l = 1$, considering typical volumes of the calorimetric cell volume and the injection of 1.5 mL and 10 μL, respectively, the concentration of ligand in syringe should be around $(10–15) \times N \times [\mathrm{M}]_0$, to guarantee that the final molar ratio $([\mathrm{L}]_\mathrm{T}/[\mathrm{M}]_\mathrm{T})$ is about 2–3 after 25–30 injections. In the case of a ligand with any size $l$ the same rule holds and the concentration of ligand in syringe should be around $(10–15) \times N/l \times [\mathrm{M}]_0$.

To check the accuracy and reliability of the calculation procedure four examples in different regions of the titration

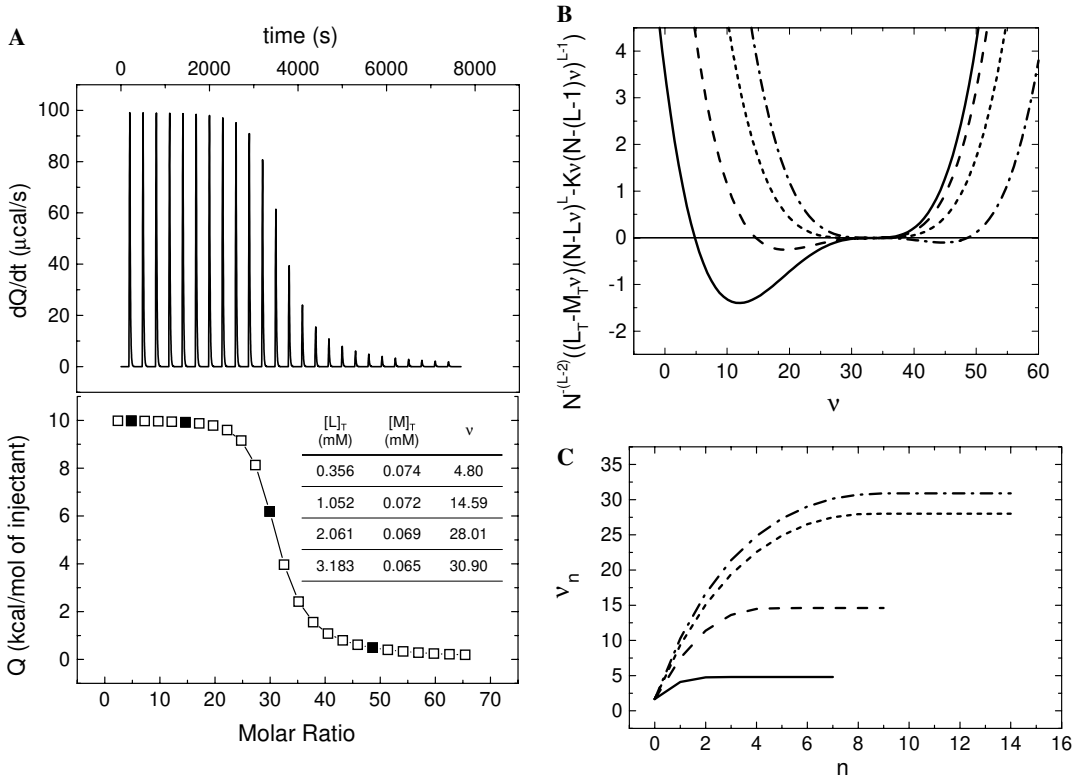


Fig. 1. (A) Simulated calorimetric titration corresponding to a macromolecule with $N = 100$ binding sites and a ligand with size $l = 3$. The calculations were done with a concentration of ligand in syringe $[L]_0 = 25$ mM, a concentration of macromolecule in the calorimetric cell $[M]_0 = 0.075$ mM, a dissociation constant $k = 10^{-5}$ M, and a binding enthalpy $\Delta H = 10$ kcal/mol. In all calculations, an injection volume $v = 10$ μL and a calorimetric cell volume $V = 1.4$ mL have been used. In the thermogram, the upper plot, the signal directly monitored in the experiment, that is, the thermal power applied by the feedback system to maintain a constant temperature irrespective of what is occurring in the cell, is shown. Each peak in the sequence corresponds to one injection of ligand into the macromolecule solution. In the lower plot the integrated area of each peak is represented as a function of the molar ratio, i.e., the ratio between the concentration of total ligand and the concentration of total macromolecule in the calorimetric cell after any injection. The thermodynamic parameters, $N$, $l$, $k$, and $\Delta H$, of a real reaction would be determined by performing a linear regression analysis of the titration plot. (B) The function $N^{-(l-2)}F(\nu)$ is plotted in four instances in the titration, corresponding to the black squares in the titration plot. The values of the total concentration of ligand and macromolecule, and the root in each case are shown in the table in A. The function $N^{-(l-2)}F(\nu)$, in this case a 4th-order polynomial, is plotted for each example: $\nu = 4.80$ (continuous line), 14.59 (dashed line), 28.01 (dotted line), and 30.9 (dashed–dotted line). There are two real positive roots; however, only one of them lies within the interval [0,100/3]. The derivative of the function $N^{-(l-2)}F(\nu)$ vanishes in one point inside the interval [0,100/3]. (C) The four sequences generated in the four calculation examples. The convergence limit value is the root determined in each case ($\nu = 4.80$, 14.59, 28.01, and 30.9) with $\varepsilon = 10^{-12}$.

plot have been selected: at low saturation ($\nu = 4.80$ and 14.59), around the equivalency point ($\nu = 28.01$), and close to complete saturation ($\nu = 30.9$). The corresponding data (the values of the total concentration of ligand and macromolecule, and the root) are indicated in the table in Fig. 1. The function $N^{-(l-2)}F(\nu)$, in this case a 4th-order polynomial, has been plotted in Fig. 1B. In any case there are two real positive roots; however, only one of them lies within the interval [0,100/3] and, therefore, possesses physical meaning. The derivative of the function $N^{-(l-2)}F(\nu)$ vanishes in one point inside the interval [0,100/3]. The recursive sequence constructed to find the root in each example is shown in Fig. 1C. The correct solution is found in less than 20 iterations using $\varepsilon = 10^{-12}$. When analyzing an experiment by nonlinear regression, both geometric parameters $N$ and $l$ should not be used simultaneously as adjustable parameters, because it would lead to a dependency value close to 1 in the fitting procedure aimed at the estimation of both parameters (that is, they would be statistically correlated). This can be seen if we rewrite Eq. (7) in terms of the normalized binding parameter $\nu/N$ (the binding density used by other authors); then, only one geometric parameter, $l$, would appear explicitly. Usually $N$ is known because it is the number of repeating units per macromolecule (e.g., number of base pairs in a nucleic acid) and it can be given a fixed value. If $N$ is not fixed in the analysis, the estimated values for $N$ and $l$ must be then understood relative to each other (although this could lead to some discrepancies as explained below).

Fig. 2 illustrates the effect of the ligand size on the calorimetric titration. Three simulated calorimetric titrations are shown, with different geometric parameters, $N$ and $l$, but sharing the same maximal number of ligand molecules bound per macromolecule or stoichiometry, $N/l = 100$. The increase in ligand size produces a reduction in the "apparent" stoichiometry, which is indicated by the localiza-

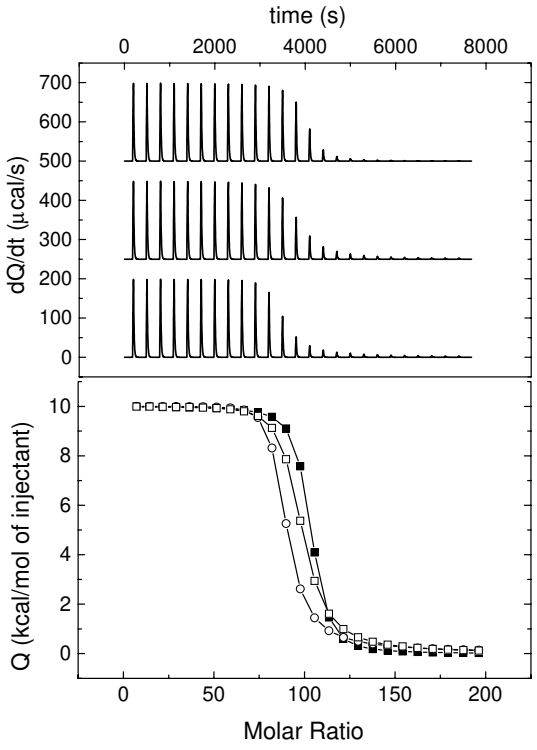


Fig. 2. Effect of the ligand size on the calorimetric titration. Three simulated calorimetric titrations: (1) macromolecule with $N = 100$ binding sites and ligand size $l = 1$ (solid squares); (2) macromolecule with $N = 200$ binding sites and ligand size $l = 2$ (open squares); and (3) macromolecule with $N = 1000$ binding sites and ligand size $l = 10$ (open circles). The calculations were done with a concentration of ligand in syringe $[L]_0 = 50$ mM, a concentration of macromolecule in the calorimetric cell $[M]_0 = 0.05$ mM, a dissociation constant $k = 10^{-5}$ M, and a binding enthalpy $\Delta H = 10$ kcal/mol. The increase in ligand size produces a reduction in the "apparent" number of binding sites (localization of the inflection point), a slight asymmetry in the titration plot, and a modification in the apparent affinity (related to the steepness of the titration).

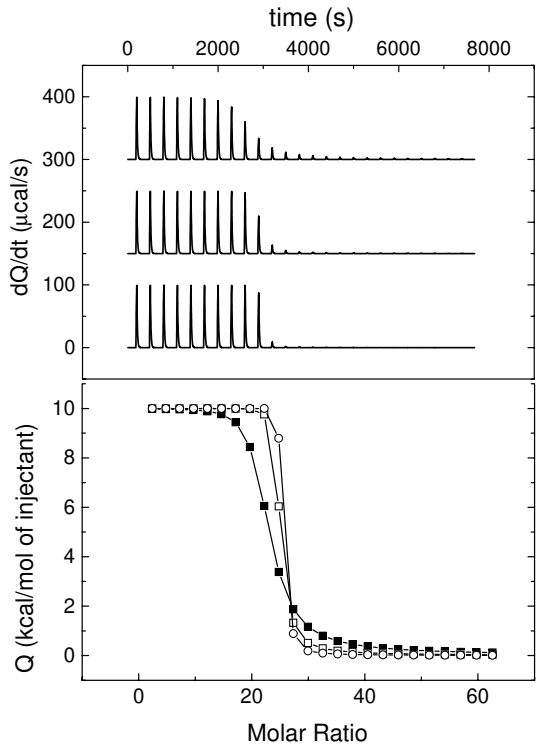


Fig. 3. Effect of the binding affinity on the calorimetric titration. Three simulated calorimetric titrations with a macromolecule with $N = 100$ binding sites and ligand size $l = 4$. Three different values for the dissociation constant were used: $k = 10^{-5}$ M (solid squares), $k = 10^{-7}$ M (open squares) and $k = 10^{-9}$ M (open circles). The calculations were done with a concentration of ligand in syringe $[L]_0 = 25$ mM, a concentration of macromolecule in the calorimetric cell $[M]_0 = 0.075$ mM, and a binding enthalpy $\Delta H = 10$ kcal/mol. The increase in binding affinity ligand size produces both an increase in the "apparent" number of binding sites (localization of the inflection point) and an increase in the slope at the inflection point.

tion of the inflection point, but the apparent binding affinity (related to the slope at the inflection point) is somewhat similar (although there is a small but significant change between $l = 1$ and $l > 1$). Moreover, Fig. 3 shows that, for given values of $N$ and $l$ (with $l > 1$), increasing or decreasing the binding affinity will change the localization of the inflection point. However, when $l = 1$ the localization of the inflection point is independent of the binding affinity. This demonstrates that the ratio $N/l$ does not define univocally the geometric features of the system but also that the values of $N$ and $l$ by themselves are important. Therefore, fixing $N$ to different values in the fitting procedure will give different sets of estimated thermodynamic parameters. This fact, the influence of the geometric parameters on the estimated thermodynamic parameters, is illustrated in Fig. 4. The titration shown in the plot was calculated with values of $N = 100$ and $l = 3$. In the fitting procedure $N$ was fixed to three different values: $N = 100$, 200, and 600, while the other parameters, $l$, $k$, and $\Delta H$, were left to vary. Although the fits obtained are indistinguishable and the estimated set of parameters are almost equivalent, there are some discrepancies in the estimated values for $l$ and k: $l$ does not exactly scale as $N$ does and the differences in the k values represent significant differences of 0.2 and 0.8 kcal/mol in the estimated binding Gibbs energies at 25 °C for $N = 200$ and $N = 600$, compared to the case with $N = 100$. The more different the selected values for $N$, the larger the discrepancies between the sets of estimated parameters. The importance of defining appropriately the geometric parameters to estimate correctly the thermodynamic parameters and to compare ligand potencies is lightened by considering that $N$ and $l$ are usually given in standard units directly related to the internal structure of the lattice-like macromolecule (e.g., in number of basepairs in nucleic acids).

Fig. 2 also shows that titrations with ligand size larger than 1 exhibit a slight asymmetry in the shape of the plot. The plot for the ligand with size $l = 1$ is symmetrical if comparing the pre-equivalency and the post-equivalency regions (that is, taking the inflection point as symmetry center), but in the plot for the ligand with size $l = 10$ the decay to zero is slower and the curvature in the post-equivalency region is lower than the curvature in the pre-equivalency region.

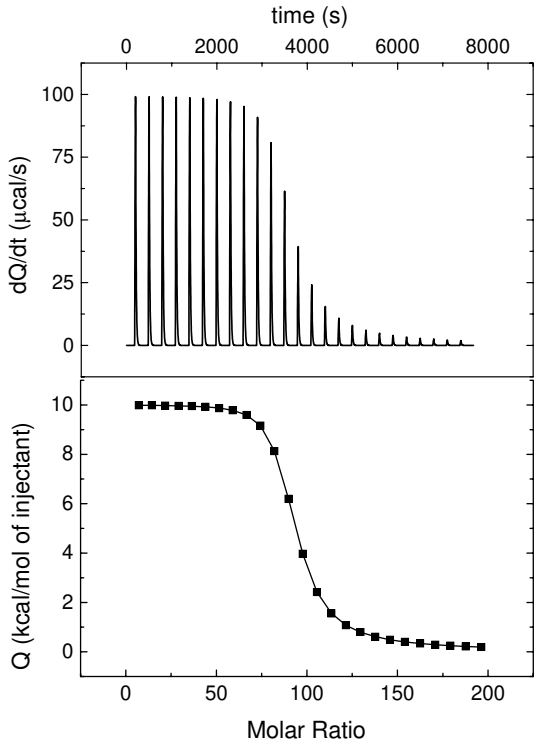


Fig. 4. Influence of the geometric parameters on the estimated thermodynamic parameters. The titration shown in the plot was calculated with a value of $N = 100$, a value of $l = 3$, a concentration of ligand in syringe $[L]_0 = 25$ mM, a concentration of macromolecule in the calorimetric cell $[M]_0 = 0.075$ mM, a dissociation constant $k = 10^{-5}$ M, and a binding enthalpy $\Delta H = 10$ kcal/mol. In the fitting procedure $N$ was fixed to three values: $N = 100$, 200, and 600. The other parameters, $l$, $k$, and $\Delta H$, were left to vary. The fits obtained in all cases are indistinguishable and the estimated parameters are almost equivalent ($N = 100$, $l = 2.99996 \pm 0.00005$, $k = 9.9998 \pm 0.0004 \cdot 10^{-6}$ M, $\Delta H = 10.0358 \pm 0.0001$ kcal/mol; $N = 200$, $l = 5.723 \pm 0.008$, $k = 1.39 \pm 0.05 \cdot 10^{-5}$ M, $\Delta H = 10.08 \pm 0.01$ kcal/mol; $N = 600$, $l = 16.39 \pm 0.03$, $k = 3.7 \pm 0.2 \cdot 10^{-5}$ M, $\Delta H = 9.99 \pm 0.01$ kcal/mol). The differences in $\Delta H$ are not important; the more significant discrepancies are in the estimated values for $l$ and $k$.

## Case II. Lineal lattice-like macromolecule with cooperative ligand binding: macromolecule with $N$ equivalent and dependent binding sites and ligand size $l \geqslant 1$

Now, bound ligands interact, favorably or unfavorably, with nearest neighbors on either side. An interaction or cooperativity parameter, $\omega$, defined as an equilibrium constant between two states (two ligands interacting side-by-side and the same two ligands not interacting and separated at least by one free macromolecule unit), represents such interaction energy. Again, a close analytical expression for the binding number has been derived [3,4]:

$$\frac{v}{[L]} = \frac{N - lv}{k}\left(\frac{(2\omega - 1)(N - lv) + v - R}{2(\omega - 1)(N - lv)}\right)^{l-1} \times \left(\frac{N - (l+1)v + R}{2(N - lv)}\right)^{2} \quad (13)$$

with:

$$R = \left((N - (l+1)v)^2 + 4\omega v(N - lv)\right)^{1/2} \quad (14)$$

Eq. (13) is never linear in $v$ (even if $l = 1$). There are two parameters affecting the shape of the Scatchard plot: $l$, which always causes an apparent negative cooperativity (positive curvature), and $\omega$, which is a truly cooperative interaction parameter and also modulates the Scatchard plot. If $0 \leqslant \omega \leqslant 1$, two ligands bound side-by-side interact unfavorably and there is negative cooperativity (positive curvature); if $1 \leqslant \omega < +\infty$, two ligands bound side-by-side interact favorably and there is positive cooperativity (negative curvature); if $\omega = 1$, two ligands bound side-by-side do not interact at all. It is obvious that at a given value of the ligand size $l$, there will be a value of the interaction parameter $\omega$ that almost compensates the negative cooperativity effect from $l$ in the Scatchard plot, resulting in a nearly linear plot. Therefore, the exclusion effect produced by ligand binding can be compensated by a higher degree of cooperativity, which might render difficult discriminating between different situations (e.g., a given ligand size could be equivalent to a larger ligand size with some positive cooperativity) [36]. Moreover, a moderate negative cooperativity is usually "absorbed" by an effective ligand size $l$ larger than the real one (that is the reason why $l$ is also called "neighbor exclusion parameter"). However, ITC allows discriminating between these two different cases, because if there is a true interaction between bound ligands, it will be reflected in an additional contribution to the overall enthalpy of binding, the interaction or cooperativity enthalpy $\Delta h$, whose effect on the titration will be observed as the binding saturation increases.

To eliminate [L] from Eq. (13), it can be rewritten expressing [L] in terms of total concentrations

$$\frac{v}{[L]_T - [M]_T v} = \frac{N - lv}{k}\left(\frac{(2\omega - 1)(N - lv) + v - R}{2(\omega - 1)(N - lv)}\right)^{l-1} \times \left(\frac{N - (l+1)v + R}{2(N - lv)}\right)^{2}. \quad (15)$$

This equation can be rewritten as

$$([L]_T - [M]_T v)(N - lv)((2\omega - 1)(N - lv) + v - R)^{l-1} \times (N - (l+1)v + R)^2 - kv(2(\omega - 1)(N - lv))^{l-1} \times (2(N - lv))^2 = 0, \quad (16)$$

which is an $(l + 3)$-order polynomial equation.

For any given values for $[L]_T$, $[M]_T$, and $k$, a root with physical meaning (i.e., positive and lower than $N/l$) can be determined. As in the previous case, the Newton–Raphson method has been used to find the root with physical meaning in the interval $[0, N/l]$. According to calculations, for any given values of $N$, $l$, $[L]_T$, $[M]_T$, $k$, and $\omega$, the correct root is obtained in less than 50 iterations with the selected accuracy.

From that, knowing $[M]_{T,i}$ and $[L]_{T,i}$ and assuming values for $N$, $l$, $k$, and $\omega$, it is possible to determine the binding

number after each injection, $v_i$, solving Eq. (15) appropriately. Then, the heat effect associated with injection, $q_i$, can be evaluated as

$$q_i = V\Big(\Delta H\Big([\mathrm{M}]_{\mathrm{T},i}v_{\mathrm{isol},i} - \Big(1-\frac{v}{V}\Big)[\mathrm{M}]_{\mathrm{T},i-1}v_{\mathrm{isol},i-1}\Big) + \Big(\Delta H + \frac{\Delta h}{2}\Big)\Big([\mathrm{M}]_{\mathrm{T},i}v_{\mathrm{sc},i} - \Big(1-\frac{v}{V}\Big)[\mathrm{M}]_{\mathrm{T},i-1}v_{\mathrm{sc},i-1}\Big) + (\Delta H + \Delta h)\Big([\mathrm{M}]_{\mathrm{T},i}v_{\mathrm{dc},i} - \Big(1-\frac{v}{V}\Big)[\mathrm{M}]_{\mathrm{T},i-1}v_{\mathrm{dc},i-1}\Big)\Big), \tag{17}$$

where $\Delta h$ is the enthalpy associated with the interaction between nearest neighbor bound ligands and $v_{\mathrm{isol}}$, $v_{\mathrm{sc}}$, and $v_{\mathrm{dc}}$ are the partial numbers of ligand molecules bound isolated, with only one nearest neighbor (singly contiguous) and with two nearest neighbors (doubly contiguous), per macromolecule, respectively. The interaction enthalpy is the enthalpy associated to the interaction between two adjacent bound ligands. Because bound ligands are indistinguishable, to prevent counting twice such interaction when evaluating the heat associated with binding using Eq. (17), the contribution of $\Delta h$ is divided by 2 in the terms corresponding to singly and doubly contiguous bound ligands. For example, if a ligand binds adjacent to an isolated bound ligand, the net enthalpy contribution is computed through the following scheme: since the net effect is that an isolated ligand disappears (gets dissociated) and two singly contiguous bound ligands appear (bind), one has to count $-\Delta H$ from the isolated ligand as if it gets dissociated and $\Delta H + \Delta h/2$ from each ligand as if they bind adjacently, with an expected net effect of $\Delta H + \Delta h$. Eq. (17) accounts for any other case, which can be explained in a similar way. The partial binding parameters can be calculated, once the total binding parameter has been determined, as

$$v_{\mathrm{isol}} = ([\mathrm{L}]_{\mathrm{T}} - [\mathrm{M}]_{\mathrm{T}}v)\frac{N-lv}{k}\left(\frac{(2\omega-1)(N-lv)+v-R}{2(\omega-1)(N-lv)}\right)^{l+1},$$

$$v_{\mathrm{sc}} = ([\mathrm{L}]_{\mathrm{T}} - [\mathrm{M}]_{\mathrm{T}}v)\frac{\omega}{\omega-1}\frac{(l-1)v-N+R}{k} \times \left(\frac{(2\omega-1)(N-lv)+v-R}{2(\omega-1)(N-lv)}\right)^{l},$$

$$v_{\mathrm{dc}} = ([\mathrm{L}]_{\mathrm{T}} - [\mathrm{M}]_{\mathrm{T}}v)\left(\frac{\omega}{2(\omega-1)}\right)^{2}\frac{((l-1)v-N+R)^2}{k(N-lv)} \times \left(\frac{(2\omega-1)(N-lv)+v-R}{2(\omega-1)(N-lv)}\right)^{l-1}, \tag{18}$$

where

$$v = v_{\mathrm{isol}} + v_{\mathrm{sc}} + v_{\mathrm{dc}}. \tag{19}$$

Eq. (18) provides information about the effect of the interaction parameter, $\omega$, on the tendency of the ligand to bind isolated or clustered. If $\omega \approx 1$ (e.g., $\omega = 0.999$), the partial numbers of ligand molecules bound per macromolecule can be evaluated for the case with no binding cooperativity. Eq. (18) is used in a nonlinear regression procedure to extract the optimal values of the thermodynamic parameters $N$, $l$, $k$, $\Delta H$, $\omega$, and $\Delta h$ from the experimental data.

Fig. 5 illustrates the effect of the cooperativity parameter on the evolution of the partial binding numbers along the titration. The calculations were done with a number of binding sites per macromolecule $N = 100$ and a ligand size $l = 4$. Four values of the cooperativity parameter have been considered: $\omega = 0$ (maximal negative cooperativity), 0.1 (negative cooperativity), 1 (no cooperativity), and 10 (positive cooperativity). In the case with no cooperativity, isolatedly bound ligands appear initially, then bound ligands with only one neighbor (singly contiguous), and later bound ligands with two neighbors (doubly contiguous). When ligands bind with positive cooperativity, isolatedly bound ligands appear initially, but immediately clustered bound ligands appear and the scene is dominated soon by the ligands bound with two neighbors. When ligands bind with negative cooperativity, isolatedly bound ligands appear initially and dominate all over the titration; the singly contiguous ligand population increases very slowly and the doubly contiguous ligand population is even less significant. When ligands bind with maximal negative cooperativity there are no ligands bound with nearest neighbors at all. This case is completely equivalent to the binding of ligands with size $l = 5$ (one unit larger) and no binding cooperativity.

In Fig. 6 the effect of a nonzero interaction enthalpy is illustrated. All plots have been drawn at the same scale for comparison. If $\Delta h$ is equal to zero, there are two differ-

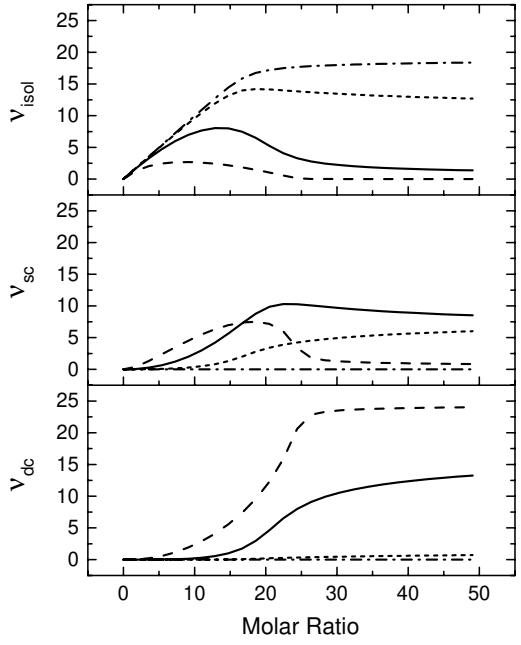


Fig. 5. Effect of the cooperativity parameter on the evolution of the partial binding numbers along the titration. The calculations were done with a number of binding sites per macromolecule $N = 100$, a ligand size $l = 4$, a concentration of ligand in syringe $[\mathrm{L}]_0 = 25$ mM, a concentration of macromolecule in the calorimetric cell $[\mathrm{M}]_0 = 0.1$ mM, a dissociation constant $k = 10^{-5}$ M, and cooperativity parameter $\omega = 0$ (dashed-dotted line), 0.1 (dotted line), 1 (continuous line), and 10 (dashed line).

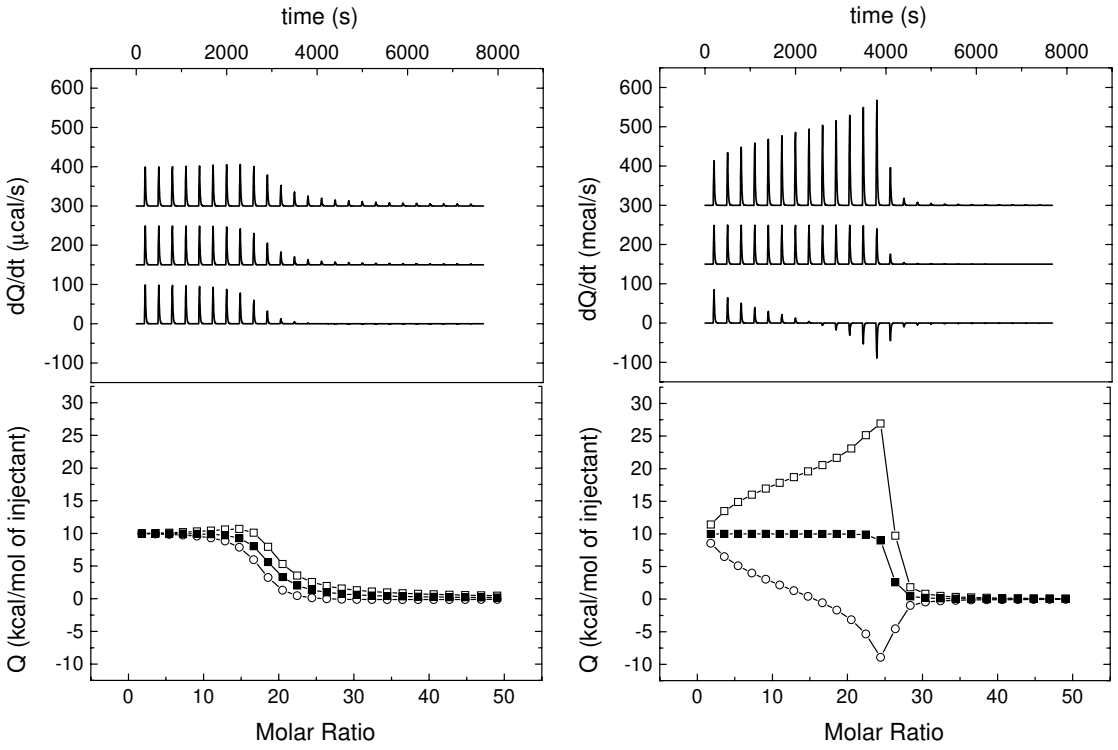


Fig. 6. Effect of the interaction enthalpy on the calorimetric titration. Simulated calorimetric titrations corresponding to a macromolecule with $N = 100$ binding sites and a ligand size $l = 4$. The calculations were done with a concentration of ligand in syringe $[L]_0 = 25$ mM, a concentration of macromolecule in the calorimetric cell $[M]_0 = 0.1$ mM, a dissociation constant $k = 10^{-5}$ M, a binding enthalpy $\Delta H = 10$ kcal/mol, cooperativity parameters $\omega = 0.1$ and 10, and interaction enthalpy $\Delta h = -10$ (open circles), 0 (closed squares) and 10 kcal/mol (open squares). (Left) Calorimetric titrations with $\omega = 0.1$ (negative cooperativity). The effect of the interaction enthalpy is small, because ligands tend to bind isolatedly; hence the heat effect reflects just the binding. (Right) Calorimetric titrations with $\omega = 10$ (positive cooperativity). The effect of the interaction enthalpy is huge, because ligands tend to bind clustered; hence the heat effect reflects both the binding event and the interaction between nearest-neighbor bound ligands.

ences between negative and positive cooperativity: unfavorable ligand–ligand interaction lowers both the apparent affinity (steepness of the titration plot) and the apparent stoichiometry (localization of the equivalency or inflection point). Thus, bearing in mind that the apparent stoichiometry is also modulated by the actual $N$ and $l$ values, without any a priori information there would be a problem to decide which case applies to the system under study (e.g., low affinity with no cooperativity would be equivalent to high affinity with negative cooperativity; small ligand size with no cooperativity would be equivalent to large ligand size with positive cooperativity). However, the presence of $\Delta h$ (which can be modified changing the experimental conditions) will help in selecting the appropriate case. If $\Delta h$ is nonzero, there is an additional contribution to the heat effect coming from the interaction between adjacently bound ligands and the different cases can be distinguished. Even if, under certain circumstances, the interaction enthalpy is zero, the enthalpy associated to any process is in general very sensitive to the environmental experimental conditions (temperature, pH, ionic strength, etc.) and, therefore, easily modulated attaining a nonzero value. This is one of the advantages of using ITC to study binding reactions. If there is negative cooperativity the effect of nonzero enthalpy is small (a slight increase or decrease of the heat effect in the preequivalency region for positive or negative interaction enthalpy, respectively), because the population of ligands bound with nearest neighbors increases very slowly as the titration proceeds (see Fig. 5). On the other hand, if there is positive cooperativity the effect of nonzero enthalpy is huge (a dramatic increase or decrease of the heat effect in the preequivalency region for positive or negative interaction enthalpy, respectively), because the population of ligands bound with at least one nearest neighbor (and preferably two nearest neighbors) dominates the titration (see Fig. 5). Another effect of a nonzero interaction enthalpy is a change in the apparent maximal binding number to lower or higher values, depending on the sign of the interaction enthalpy.

More information on the interaction or cooperativity thermodynamic parameters can be obtained by performing reverse titrations [7,31,37]. In a direct titration the ligand is injected into a macromolecule solution, whereas in a reverse titration the macromolecule is injected into a ligand solution. If the stoichiometry is 1:1, no differences should arise between these two experiments. However, if the stoichiometry is not 1:1 and the binding sites are not equivalent and/or independent, the comparison of both experiments reveals substantial differences. Fig. 7 shows direct (left) and reverse (right) calorimetric titrations with and without

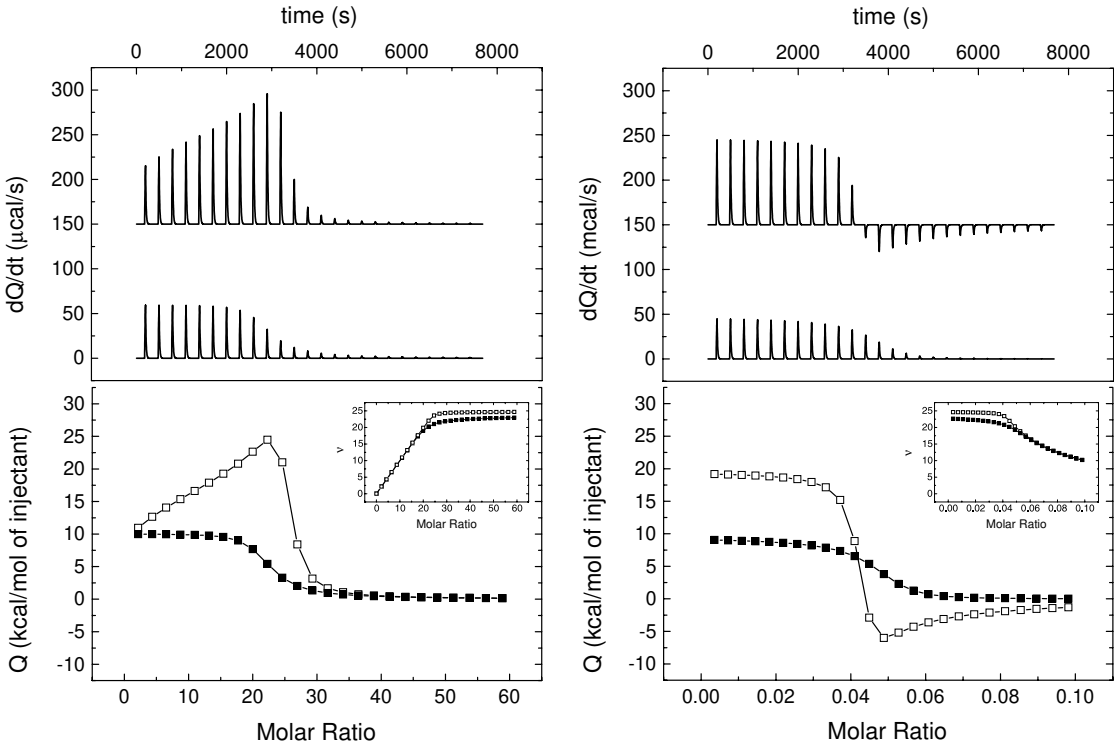


Fig. 7. Comparison between direct titrations (ligand into macromolecule solution; left) and reverse titrations (macromolecule into ligand solution; right). Simulated calorimetric titrations corresponding to a macromolecule with $N = 100$ binding sites and a ligand size $l = 4$. For the direct titrations, a concentration of ligand in syringe $[L]_0 = 15$ mM and a concentration of macromolecule in the calorimetric cell $[M]_0 = 0.05$ mM were employed. For the reverse titrations, a concentration of ligand in the calorimetric cell $[L]_0 = 1$ mM and a concentration of macromolecule in the syringe $[M]_0 = 0.5$ mM were employed. A dissociation constant $k = 10^{-5}$ M, a binding enthalpy $\Delta H = 10$ kcal/mol, cooperativity parameter $\omega = 0$ (closed squares) and 5 (open squares) (negative cooperativity has not been simulated, because it causes a small effect, as demonstrated in Fig. 6), and interaction enthalpy $\Delta h = 0$ and 10 kcal/mol were used. To calculate the normalized heat in each injection per mole of injectant, in the case of the reverse titration it was normalized per mole of binding sites injected, that is, dividing the heat per injection by $v \times [M]_0 \times N/l$. In the insets, the evolution of the number of ligand molecules bound per macromolecule, $v$, is plotted as a function of the molar ratio. The molar ratio is always defined as the quotient between the total concentration of the reactant injected and the total concentration of the reactant in the calorimetric cell.

ligand cooperativity. To simulate the reverse titrations the roles of the ligand and macromolecule are exchanged in Eq. (11), but all other equations remains unaltered. In the initial stages of a direct titration the macromolecule is in excess and the ligand is at a subsaturating concentration. As the titration proceeds, the ligand reaches higher concentrations and the macromolecule becomes saturated, the number of ligand molecules bound per macromolecule increases (see inset), the number of ligands isolatedly bound per macromolecule decreases, and the number of ligands doubly contiguous increases. On the other hand, in the initial stages of a reverse titration the ligand is in excess and the macromolecule becomes almost saturated at the beginning, and, therefore, most of the ligands bound present nearest neighbors (singly and doubly contiguous). As the titration proceeds, the macromolecule reaches higher concentrations and the ligand subsaturating concentrations. Consequently, the increase in macromolecule concentration induces ligand dissociation. Then, some of the bound ligands with nearest neighbors get dissociated to bind with fewer neighbors. Therefore, the number of ligand molecules bound per macromolecule decreases (see inset), the number of ligands isolatedly bound increases, and the number of ligands doubly contiguous decreases. If there is no cooperativity, there are no important differences between the direct and the reverse titration. However, if there is cooperativity, there are dramatic differences between both experiments: the increase in the heat per injection in the direct titration reflects the progressive increase in ligands bound with nearest neighbors; the decrease in the heat per injection in the direct titration, even to negative values when both enthalpies $\Delta H$ and $\Delta h$ are positive, reflects the progressive increase in ligands bound with fewer neighbors and the dissociation induced by the increase in macromolecule concentration.

## Conclusions

McGhee–von Hippel theory for cooperative ligand binding to one-dimensional homogeneous lattice-like macromolecules has been implemented in isothermal titration calorimetry. Although the formalism is based on the Scatchard representation, the method is exact and rigorous, without the weaknesses and drawbacks intrinsic to the Scatchard analysis, and it can be employed in any titration technique (e.g., spectroscopy) in which the only indepen-

dent variables are the total concentrations of reactants. The method implies solving numerically an $(l+3)$-order or an $(l+1)$-order polynomial equation (where $l$ is the ligand size in repeating macromolecule units), depending on whether cooperative binding is considered. Therefore, it is shown how numerical methods can be used to extend the applicability of biophysical techniques to more complex systems. Extensions for heterogeneous lattice-like macromolecules (e.g., finite lattices, nonhomogeneous distribution of binding sites, or different classes of binding sites in the macromolecule) can be easily performed.

This methodology permits the study of binding reactions with long one-dimensional macromolecules by ITC, which has been scarcely used for this type of system. Thus, it will be possible to take advantage of the benefits from using this technique. ITC allows determining simultaneously the affinity and the enthalpy of binding, discriminating between intrinsic parameters ($k$ and $\Delta H$) and interaction or cooperativity parameters ($\omega$ and $\Delta h$). Therefore, it provides a complete thermodynamic characterization of the binding process (Gibbs energy, enthalpy, entropy, and stoichiometry). In addition, having affinity and enthalpy determined simultaneously, and the possibility of modulating them by changing the experimental conditions, gives us an additional element with which to extract valuable information and to discriminate among different possible cases applicable to the system under study. The comparison between reverse and direct titrations gives additional information about cooperativity phenomena. An analysis of the effect of the different binding parameters, geometric and thermodynamic, on the calorimetric titration has been presented. On the other hand, limitations intrinsic to ITC should be bore in mind (e.g., kinetic effects arising in slow binding reactions).

## Acknowledgments

A.V.C is a recipient of a Ramón y Cajal Research Contract from the Spanish Ministry of Science and Technology. This research was funded by Grant SAF2004-07722 from the Spanish Ministry of Education and Science.

## References

[1] C.R. Cantor, P.R. Schimmel, Biophysical chemistry, Part III: The behaviour of biological macromolecules, W.H. Freeman, New York, USA, 1980.
[2] G. Scatchard, The attraction of proteins for small molecules and ions, Ann. NY. Acad. Sci. 51 (1949) 660–672.
[3] J.D. McGhee, P.H. von Hippel, Theoretical aspects of DNA–protein interactions: co-operative and non-co-operative binding of large ligands to a one-dimensional homogeneous lattice, J. Mol. Biol. 86 (1974) 469–489.
[4] J.D. McGhee, P.H. von Hippel, Erratum. Theoretical aspects of DNA–protein interactions: co-operative and non-co-operative binding of large ligands to a one-dimensional homogeneous lattice, J. Mol. Biol. 103 (1976) 679.
[5] J.B. Chaires, Analysis and interpretation of ligand–DNA binding isotherms, Methods Enzymol. 340 (2001) 3–22.
[6] I.R. Epstein, Cooperative and non-cooperative binding of large ligands to a finite one-dimensional lattice. A model for ligand-oligonucleotide interactions, Biophys. Chem. 8 (1978) 327–339.
[7] O.V. Tsodikov, J.A. Holbrook, I.A. Shkel, M.T. Record Jr., Analytic binding isotherms describing competitive interactions of a protein ligand with specific and nonspecific sites on the same DNA oligomer, Biophys. J. 81 (2001) 1960–1969.
[8] A. Kristiansen, K.M. Vårum, H. Grasdalen, Quantitative studies of the non-productive binding of lysozyme to partially N-acetylated chitosans, Biochim. Biophys. Acta 1425 (2001) 137–150.
[9] G. Schwarz, S. Stankowski, Linear cooperative binding of large ligands involving mutual exclusion of different binding modes, Biophys. Chem. 10 (1979) 173–181.
[10] S. Rajendran, M.J. Jezewska, W. Bujalowski, Human DNA polymerase beta recognizes single-stranded DNA using two different binding modes, J. Biol. Chem. 273 (1998) 31021–31031.
[11] N. Dattagupta, M. Hogan, D.M. Crothers, Interaction of Netropsin and Distamycin with deoxyribonucleic acid: electric dichroism study, Biochemistry 19 (1980) 5998–6005.
[12] J.B. Chaires, Allosteric conversion of Z DNA to an intercalated right-handed conformation by Daunomycin, J. Biol. Chem. 261 (1986) 8899–8907.
[13] W. Bujalowski, T.M. Lohman, A general method of analysis of ligand-macromolecule equilibria using a spectroscopic signal from the ligand to monitor binding. Application to *Escherichia coli* single-strand binding protein–nucleic acid interactions, Biochemistry 26 (1987) 3099–3106.
[14] T.M. Lohman, W. Bujalowski, Thermodynamic methods for model-independent determination of equilibrium binding isotherms for protein–DNA interactions: spectroscopic approaches to monitor binding, Methods Enzymol. 208 (1991) 258–290.
[15] T. Wiseman, S. Williston, J.F. Brandts, L.N. Nin, Rapid measurement of binding constants and heats of binding using a new titration calorimeter, Anal. Biochem. 179 (1989) 131–137.
[16] E. Freire, O.L. Mayorga, M. Straume, Isothermal titration calorimetry, Anal. Chem. 62 (1990) 950A–959A.
[17] M. El Harrous, A. Parody-Morreale, Measurement of biochemical affinities with a Gill titration calorimeter, Anal. Biochem. 254 (1997) 96–108.
[18] I. Jelessarov, H.R. Bosshard, Isothermal titration calorimetry and differential scanning calorimetry as complementary tools to investigate the energetics of biomolecular recognition, J. Mol. Recogn. 12 (1999) 3–18.
[19] S. Leavitt, E. Freire, Direct measurement of protein binding energetics by isothermal titration calorimetry, Curr. Opin. Struct. Biol. 11 (2001) 560–566.
[20] W.H. Ward, G.A. Holdgate, Isothermal titration calorimetry in drug discovery, Prog. Med. Chem. 38 (2001) 309–376.
[21] A. Velazquez-Campoy, E. Freire, Isothermal titration calorimetry: measuring intermolecular interactions, in: S. Richard Simpson (Ed.), Proteins and Proteomics, A Laboratory Manual, Cold Spring Harbor Laboratory Press, New York, USA, 2003, pp. 882–892.
[22] A. Velazquez-Campoy, H. Ohtaka, A. Nezami, S. Muzammil, E. Freire, Isothermal Titration Calorimetry, in: J.S. Bonifacino, M. Dasso, J.B. Harford, J. Lippincott-Schwartz, K.M. Yamada (Eds.), Current Protocols in Cell Biology: Macromolecular Interactions, John Wiley & Sons, New York, USA, 2004.
[23] A. Velazquez-Campoy, S.A. Leavitt, E. Freire, Characterization of protein-protein interactions by isothermal titration calorimetry, Methods Mol. Biol. 261 (2004) 35–54.
[24] A. Velazquez-Campoy, E. Freire, ITC in the post-genomic era...? Priceless, Biophys. Chem. 115 (2005) 115–124.
[25] T. Ohyama, J.A. Cowan, An approach to the evaluation of RNA solution structure and metal coordination chemistry by titration calorimetry, J. Biol. Inorg. Chem. 1 (1996) 83–89.
[26] T. Ohyama, J.A. Cowan, Influence of monovalent cations on magnesium binding to poly-RNA by solution titration calorimetry:

an analysis of the salt dependence of binding enthalpies and entropies, J. Biol. Inorg. Chem. 1 (1996) 111–116.
[27] T. Lundbäck, T. Härd, Salt dependence of the free energy, enthalpy, and entropy of nonsequence specific DNA binding, J. Phys. Chem. 100 (1996) 17690–17695.
[28] T. Lundbäck, H. Hansson, S. Knapp, R. Ladenstein, T. Härd, Thermodynamic characterization of non-sequence-specific DNA-binding by the Sso7d protein from *Sulfolobus solfataricus*, J. Mol. Biol. 276 (1998) 775–786.
[29] M.M. Lopez, K. Yutani, G.I. Makhatadze, Interactions of the major cold shock protein of *Bacillus subtilis* CspB with single-stranded DNA templates of different base composition, J. Biol. Chem. 274 (1999) 33601–33608.
[30] K. Utsuno, Y. Maeda, M. Tsuboi, et al., How and how much can Hoechst 33258 cause unwinding in a DNA duplex? Chem. Pharm. Bull. 47 (1999) 1363–1368.
[31] J.A. Holbrook, O.V. Tsodikov, R.M. Saecker, M.T. Record Jr., Specific and non-specific interactions of integration host factor with DNA: thermodynamic evidence for disruption of multiple IHF surface salt-bridges coupled to DNA binding, J. Mol. Biol. 310 (2001) 379–401.
[32] M. Girard, S.L. Turgeon, S.F. Gauthier, Thermodynamic parameters of β-lactoglobulin-pectin complexes assessed by isothermal titration calorimetry, J. Agric. Food Chem. 51 (2003) 4450–4455.
[33] E. Di Cera, Y. Kong, Theory of multivalent binding in one and two-dimensional lattices, Biophys. Chem. 61 (1996) 107–124.
[34] W. Bujalowski, T.M. Lohman, C.F. Anderson, On the cooperative binding of large ligands to a one-dimensional homogeneous lattice: The generalized three-state lattice model, Biopolymers 28 (1989) 1637–1643.
[35] W.H. Press, B.P. Flannery, S.A. Teukolsky, W.T. Vetterling, in: Numerical Recipes in C: The Art of Scientific Computing, Cambridge University Press, New York, NY, 1992, pp. 362–368.
[36] G. Schwarz, On the analysis of linear binding effects associated with curved Scatchard plots, Biophys. Chem. 6 (1976) 65–76.
[37] S.C. Kowalczykowski, L.S. Paul, N. Lonberg, J.W. Newport, J.A. McSwiggen, P.H. von Hippel, Cooperative and noncooperative binding of protein ligands to nucleic acid lattices: experimental approaches to the determination of thermodynamic parameters, Biochemistry 25 (1986) 1226–1240.